Soil-structure interaction analysis using a 1DT-3C wave propagation model

Reine Fares, Maria Paola Santisi D'avila, Anne Deschamps

Soil-Structure Interaction analysis using a 1DT-3C wave propagation model

Reine Fares[1,2], Maria Paola Santisi d'Avila[1], Anne Deschamps[2]

[1] Université Côte d'Azur, CNRS, LJAD, 06108 Nice, France.

[2] Université Côte d'Azur, CNRS, IRD, OCA, Géoazur, 06560 Valbonne, France.

Corresponding author:

Reine Fares

Laboratoire J. A. Dieudonné, Université Côte d'Azur

28, Avenue Valrose - 06108 Nice - France

Email: reine.fares@unice.fr

ABSTRACT

The soil-structure interaction (SSI) is generally neglected for seismic design of ordinary buildings. A modeling technique is proposed to facilitate the integration of SSI in building design, considering rocking effects and the shallow foundation deformability. The proposed technique is suitable when the soil can be considered as horizontally layered. The one-directional three-component wave propagation is numerically simulated in a T-shaped horizontally layered soil domain assembled with a three-dimensional (3D) frame structure. A 3D soil model is used until a fixed depth and a 1D model is supposed to be a sufficient approximation in deeper soil layers. The 1DT-3C wave propagation approach is inspired by the consideration that SSI is detected in the near-surface soil layers. The proposed modeling approach is verified by comparison with a fully 3D model for vertical propagation in horizontally layered soil and periodic lateral boundary condition. The 1DT-3C wave propagation modeling technique is used to investigate the building response and SSI effects that vary with the frequency content of seismic loading and building-to-soil frequency ratio, respectively.

Keywords: Soil-structure interaction; finite element method; seismic load; wave propagation; three-component motion; nonlinear behavior.

1. INTRODUCTION

The free-field (FF) motion is currently used as seismic loading at the bottom of a fixed-base (FB) building, for structural design of buildings with shallow foundation, according to European seismic design provisions [1]. According to Saez *et al.* [2], the two-step analysis does not permit to numerically simulate the soil-structure interaction (SSI) that modifies the structural seismic

response, influenced by structural dynamic features, soil mechanical parameters and input motion characteristics. According to Mylonakis and Gazetas [3], an increase in the fundamental period of a structure due to SSI does not necessarily lead to smaller response and considering SSI as beneficial is an oversimplification which may lead to unsafe design. A one-step analysis (Saez *et al.* [2]), where the dynamic equilibrium problem is solved directly for the assembly of soil domain and structure at the surface, allows the simulation of the seismic response of soil and structure taking into account the SSI effects.

Stewart *et al.* [4] express inertial interaction effects for buildings in terms of lengthening of the first-mode period (flexible-base to fixed-base first-mode period ratio higher than one). According to Saez *et al.* [2], SSI effects exist when the seismic response obtained by solving the dynamic equilibrium problem applied to the assembly of soil domain and frame structure (one-step analysis) is strongly different from that obtained by imposing the free-field motion at the base of the fixed-base structure (two-step analysis).

Jennings and Bielak [5], using simplified numerical models, show that the effect of SSI on the seismic response of buildings occurs predominantly in the direction of the fundamental mode shape. Moreover, the effects of interaction may be negligible for higher modes in the case of tall buildings having a translational first mode shape (of the fixed base structure).

Three-dimensional (3D) wave propagation models have been proposed to obtain the six components of motion in the soil, where the dynamic equilibrium problem is solved directly for the assembly of structure and the 3D soil domain (such as the NRC ESSI simulator, according to Jeremic *et al.* [6] and Coleman *et al.* [7]). This allows taking into account the propagation of body and surface waves and, at the same time, the spatial variability of the stratigraphy, rocking effect and the interaction with the foundation.

Despite the evolution of 3D numerical models, major uncertainties concerning the geotechnical model, difficulties related with the absorbing condition at the lateral boundaries, added to the high computational cost of an extended 3D mesh make this kind of approach unusable for ordinary building design.

Santisi d'Avila and Lopez Caballero [8] provide a modeling technique for building design, taking into account SSI. The one-directional propagation of a three-component earthquake in a horizontally layered soil (1D-3C approach), having nonlinear behavior and a 3D frame building at the surface, is numerically simulated in a finite element scheme. The dynamic equilibrium equation is solved directly for the assembly of soil domain and one building (one-step analysis), using three-node line FE for soil with axial and shear strains in the horizontal plan imposed equal to zero in the strain vector (without need of tie constraint). When the hypotheses of horizontally layered soil and vertical propagation are suitable, the 1D-3C wave propagation approach for SSI can be used with the advantage that geotechnical parameters are easy to characterize for a one-dimensional soil model (using a single borehole investigation), boundary condition definition is simple (the input signal and the absorbing boundary condition are given for only one element), and the computation time is reduced compared with a 3D soil model. The 1D-3C wave propagation approach for SSI assumes rigid shallow foundation (the bases of building columns are connected by a membrane rigid link) and reduced rocking effects (the same three-component motion at the soil surface is applied at the base of all building columns). The 1D-3C wave propagation approach is not suitable for structure-soil-structure interaction (SSSI) analysis.

This research provides a modeling technique for building design, taking into account SSI and eventually SSSI, using any commercial finite element (FE) code, under the assumption of

horizontally layered soil and vertical propagation. Abaqus software has been used in this study. A fully 3D soil domain is modeled until a fixed depth and a one-dimensional model is used for deeper layers. Using the 1DT-3C wave propagation approach, the foundation deformability and rocking effects can be taken into account in SSI and SSSI analyses.

The 1DT-3C wave propagation modeling technique for SSI analysis is verified by comparison with a fully 3D soil model for vertical propagation in a horizontally layered soil and periodic lateral boundary condition.

2. 1D-3C WAVE PROPAGATION MODEL FOR SSI ANALYSIS

A first study has been undertaken to reproduce the 1D-3C wave propagation approach for SSI proposed by Santisi d'Avila and Lopez Caballero [8], using any commercial FE code. Abaqus software has been used in this research.

The soil profile is assumed as horizontally layered and infinitely extended along the horizontal directions x and y, according to the xyz coordinate system represented in Fig. 1. Consequently, no strain variation is considered in these directions. Shear and pressure waves propagate vertically in z-direction from the top of the underlying elastic bedrock to the soil surface. The soil is assumed to be a continuous and homogeneous medium, with nonlinear constitutive behavior.

The discrete dynamic equilibrium equation for the assembly of soil domain and frame structure, including compatibility conditions, three-dimensional nonlinear constitutive relation and the imposed boundary conditions, is solved directly (one-step analysis).

All the proposed modeling techniques, in this research, can be adopted independently of the constitutive relationship selected for soil and structure.

2.1. Spatial discretization of soil domain and boundary conditions

The hypothesis of vertical propagation in a horizontally layered soil allows the one-dimensional spatial discretization of the soil domain. The soil is modeled using 20-node solid FE, having three translational degrees of freedom per node. A periodic lateral boundary condition is imposed at the lateral boundaries in the soil domain, to impose zero stains ε_x and ε_y, using a tie constraint between lateral surfaces. According to Zienkiewicz *et al.* [9] and Saez *et al.* [2], this condition is verified because the lateral limits of the problem are considered to be far enough from the structure.

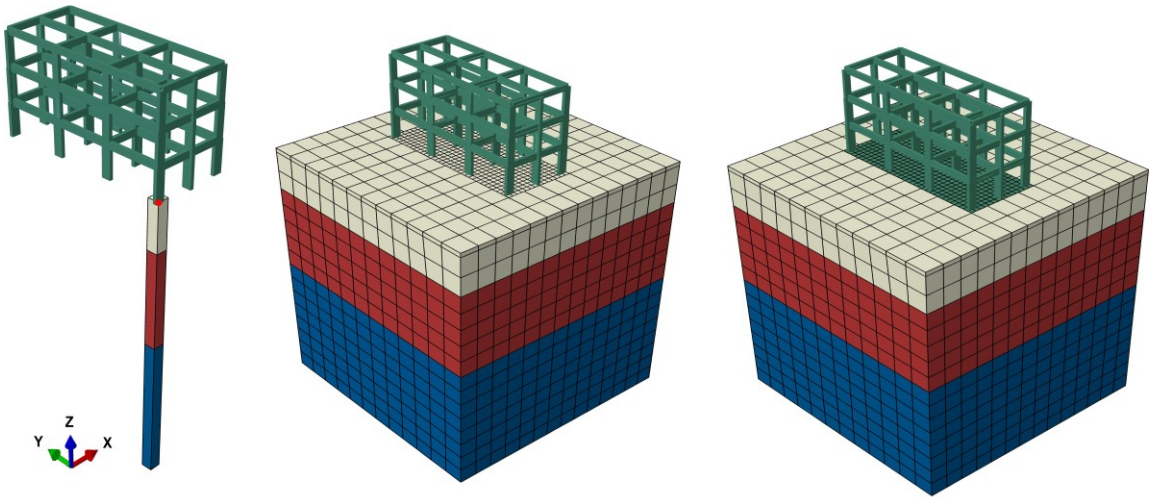

(a) (b) (c)

Fig. 1. Assembly of a frame structure and a multilayer soil domain shaken by a three-component seismic motion, for SSI analysis: (a) 1D-3C wave propagation model, where the assembly is done in only one node; (b) 3D-3C wave propagation model, with connection node-to-node between building and soil; (c) 3D-3C model, where the foundation is modeled and embedded in the soil domain.

The minimum number of quadratic solid elements per layer is defined as $p\,f\,h_i/\left(2v_{si}\right)$, where h_i is the thickness of the i-th layer and v_{si} is the shear wave velocity in the medium, this latter related to the minimum wavelength of the seismic signal by the ratio v_{si}/f. The maximum frequency, above which the spectral content of the input signal can be considered negligible, is fixed as $f=15\,\mathrm{Hz}$. The minimum number of nodes per wavelength, to accurately represent the seismic signal, is assumed as the maximum between $p=2v_{si}/f$ (almost one element every meter) and $p=10$.

The soil column is bounded at the bottom by a semi-infinite bedrock having elastic behavior. A linear viscous dashpot is localized at the bottom of the soil column, in each direction of motion, as absorbing boundary condition (as adopted by Joyner and Chen [10] and Santisi d'Avila and Lopez Caballero [8]), to take into account the finite rigidity of the bedrock and allow energy to be radiated back into the underlying medium. The seismic loading is applied at the soil-bedrock interface in terms of force. According to the applied boundary condition, the shear and normal stresses at the soil column base, at the bedrock interface, are $\rho_b\,v_{sb}\left(v_x-2v_{bx}\right)$, $\rho_b\,v_{sb}\left(v_y-2v_{by}\right)$ and $\rho_b\,v_{pb}\left(v_z-2v_{bz}\right)$, respectively. The parameters ρ_b, v_{sb} and v_{pb} are the bedrock density and shear and compressional wave velocities in the bedrock, respectively. The three components of the incident seismic motion at the bedrock level in terms of velocity v_{bx}, v_{by} and v_{bz}, in x-, y- and z-direction, respectively, can be obtained by halving the seismic motion at the outcropping bedrock. The three terms v_x, v_y and v_z are the unknown velocities (incident and reflected motion), at the soil-bedrock interface, in x-, y- and z-direction, respectively, that are evaluated during the process.

In the 1D-3C wave propagation approach for SSI, the solid FE have unit area in the horizontal plan (Fig. 1a). In a 1D wave propagation model, the area of the soil column A appears as a constant in each term of the equilibrium equation, i.e. in the mass, stiffness and damping matrices and in the seismic loading vector. Consequently, in the FF case the soil motion can be correctly obtained even if a unit area is adopted. This is not the case in SSI analyses where the area of the soil domain A, concerned by interaction effects, have to be taken into account in the balance. In a commercial FE code, the area of the soil domain A can be considered by imposing a soil density of ρA and an elasticity modulus in compression of $E_0 A$ to correctly define the mass and stiffness of soil part, where ρ and E_0 are the soil density and elasticity modulus in compression, respectively.

The damping coefficient of dashpots imposed at each node of the soil column base is $\rho_b v_{sb} A_i$ for those in the horizontal directions and $\rho_b v_{pb} A_i$ in the vertical direction. $A_i = A/n$ is the influence area of each node and n is the number of nodes at the soil-bedrock interface.

The seismic loading components, applied at the bottom of the soil column in terms of force, are $(\rho_b v_{sb} A_i) 2v_{bx}$, $(\rho_b v_{sb} A_i) 2v_{by}$ and $(\rho_b v_{pb} A_i) 2v_{bz}$.

2.2. Soil constitutive relationship

The Iwan's 3D elasto-plastic model with kinematic hardening (Joyner and Chen [10], Iwan [11], Joyner [12]) is adopted for soils in the proposed model in Abaqus software. The Iwan's model satisfies the Masing's criteria (Kramer [13]) and does not depend on the number of loading cycles. According to Joyner [12], the tangent constitutive matrix is deduced from the actual strain level and the strain and stress values at the previous time step. The stress increment is evaluated at each time step. The stress level depends on the strain increment and strain history

but not on the strain rate. Therefore, this rheological model has no viscous damping. The energy dissipation process is purely hysteretic and does not depend on the frequency.

The rheological formulation is in terms of total stresses. The plasticity model uses von Mises yield surface that assumes pressure-independent behavior, that means yielding is independent of the average pressure stress. This assumption is acceptable for dry and undrained soil.

The main feature of Iwan's model is that the mechanical parameters to calibrate the rheological model are easily obtained from laboratory dynamic tests on soil samples. The size of the yield surface is imposed by the backbone curve in the uniaxial stress case. In this research, the Poisson's ratio is assumed constant during the time history and, consequently, the normalized decay curve of the elastic modulus in compression is $E/E_0 \simeq$. The same shear modulus decay curve is used for all shear components.

An isotropic-kinematic hardening model is used to simulate the inelastic material behavior subjected to cyclic loading. The kinematic hardening model is linearly performed at a constant hardening rate to approximate the hardening behavior described by Prager hardening rule. The plasticity model assumes associated plastic flow, allowing isotropic yielding. Therefore, as the material yields, the inelastic deformation rate is in the direction of the normal to the yield surface (the plastic deformation is volume invariant).

The nonlinear behavior is characterized in Abaqus software providing the uniaxial first loading curve in terms of axial stresses and strains, deduced by the compressive modulus reduction curve. If resonant column tests provide shear modulus decay curves $G/G_0(\gamma)$, the demanded first loading curve is evaluated as $\sigma(\varepsilon) = E/E_0(\varepsilon) E_0 \varepsilon$, where the axial stress $\sigma(\varepsilon)$ can be calculated from shear stress $\tau(\gamma)$ as $\sigma(\varepsilon) = \sqrt{3}\,\tau(\gamma)$, $E/E_0(\varepsilon)$ is the normalized decay curve of

elastic modulus in compression versus axial strain ε that is assumed equal to $G/G_0(\gamma)$ and $\varepsilon = \sqrt{3}\,\gamma\, G_0/E_0$. In the present study, the soil behavior is assumed adequately described by a hyperbolic stress-strain curve (Hardin and Drnevich [14]). This assumption yields a normalized shear modulus decay curve, expressed as $G/G_0 = 1/\left(1+|\gamma/\gamma_r|\right)$, where γ_r is a reference shear strain corresponding to an actual tangent shear modulus equivalent to 50% of the elastic shear modulus, in a normalized shear modulus decay curve provided by laboratory test data.

In the following analysis, the shear modulus reduction curve shown in Fig. 2 is adopted to simulate the nonlinear soil response. Fig. 3 shows stress-strain loops in the cases of 1-, 2- and 3-Component loading, obtained using the plasticity model implemented in Abaqus, for the input shear strain time history in Fig. 2. The backbone curve is discretized using 98 intervals, and the nonlinear kinematic hardening with ratcheting is modeled using 10 backstresses (kinematic shift of the yield surface).

As discussed by Santisi d'Avila *et al*. [15], the shear strength is reduced for 2C and 3C loading, compared with the uniaxial case (Fig. 3).

The backbone curve is corrected as $\sigma(\varepsilon) = E/E_0(\varepsilon)(E_0\, A)\varepsilon$ to consider the soil domain surface A, in the case of the 1D-3C wave propagation model for SSI analyses (where unit-area solid finite elements are used for soil), undertaken using a commercial FE code as Abaqus.

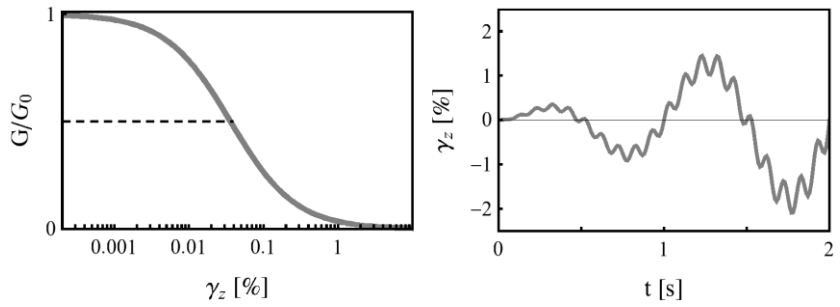

Fig. 2. Shear modulus decay curve (left) and input shear strain time history (right).

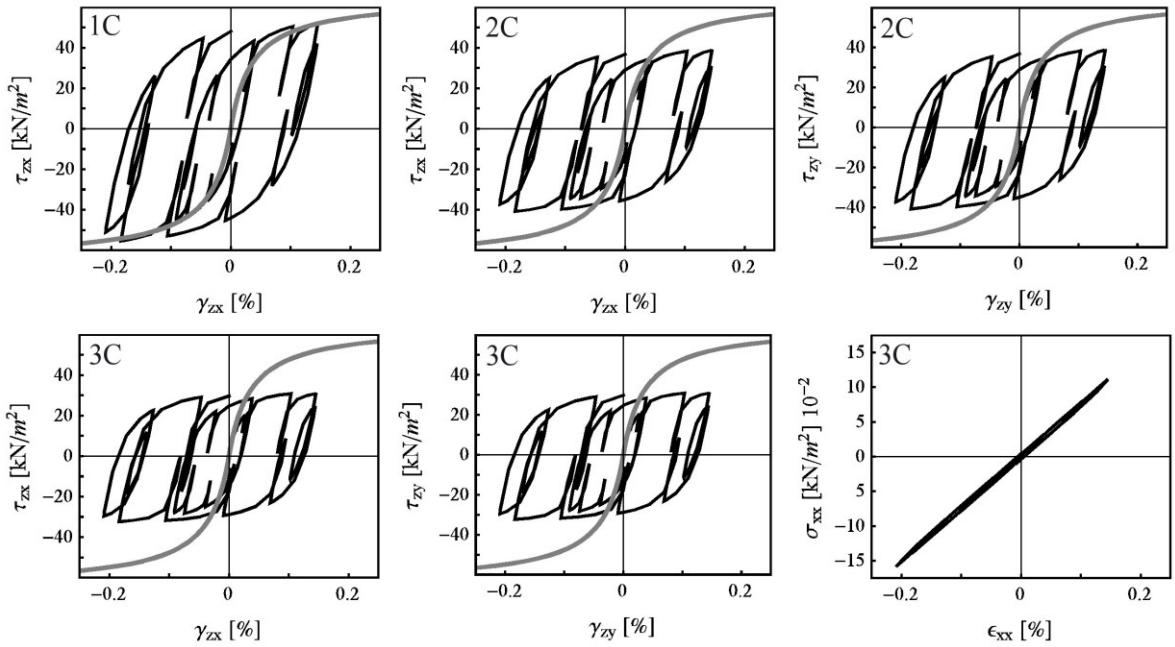

Fig. 3. The backbone curve for one-component loading and hysteresis loops in a unit cube of soil loaded by a 1-, 2- and 3-Component strain (1C, 2C and 3C, respectively). The input strain components have the same time history.

2.3. Building model and building-soil system

The 3D frame structure is modeled using Timoshenko beam elements having six degrees of freedom per node. The transverse shear stiffness χGA of the beam cross-section is defined using a shear correction factor (Kaneko [16]) equal to $\chi = (5(1+\nu))/(6+5\nu)$. A linear constitutive behavior is assumed for the structure.

The damping provided by non-structural components is taken into account according to Rayleigh approach (Chopra [17]). In fact, the damping submatrix related to the building is assumed as mass and stiffness proportional, using coefficients dependent on the first two fixed-base natural frequencies.

Live and dead loads are imposed on the beams in terms of mass per unit length.

The base of building columns are all connected by a membrane rigid link under the assumption of rigid shallow foundation. According to the 1D-3C wave propagation approach, the building is rigidly connected at the bottom to the soil surface. Rotational degrees of freedom of nodes at the base of columns are blocked.

In the 3D model in Fig. 1b, a rigid link imposed between the different column bases, directly assembled with the soil, implies that the same horizontal motion is transmitted at each building column base. Consequently, the 1D-3C wave propagation model (Fig. 1a) and the 3D model with connection node-to-node between building and soil shown in Fig. 1b are equivalent. According to the adopted constitutive model for soil, the effect of initial conditions in terms of confining pressure in the soil is not influent in the total stress analysis.

The advantages of the 1D-3C wave propagation approach for SSI are that modelling difficulties and computation time are reduced compared with a 3D soil model. In fact, geotechnical parameters are easy to characterize for a one-dimensional soil model (using a single borehole investigation) and boundary condition definition is simple (the input signal and the absorbing boundary condition are given for only one element. Moreover, the mesh is considerably reduced (Fig.1).

2.4. Time discretization

The dynamic process is solved step-by-step by the implicit Hilber-Hughes-Taylor algorithm (Hughes [18]), also called α-method. The three parameters $\alpha = -0.1$, $\beta = 0.25(1-\alpha)^2 = 0.3025$ and $\gamma = 0.5 - \alpha = 0.6$ guarantee an unconditionally numerical stability of the time integration scheme and numerical damping to reduce high frequency content, without having any significant effect on the meaningful, lower frequency response. The dynamic equilibrium equation is

directly solved using a time step between $dt = 10^{-4}$ s and the time step used for the input signal sampling. The building weight and gravity load are imposed as static initial condition in terms of strain and stress.

2.5. Soil domain area concerned by the SSI

The simulation of SSI effects requires the representation of an adequate soil volume. The soil depth is imposed by the position of the soil-bedrock interface, where the incident motion is imposed.

According to Santisi d'Avila and Lopez Caballero [8], a procedure to identify the soil domain area is adopted, taking into account implicitly all the parameters influencing its choice, as for example the foundation size and the participant mass of soil and building associated to the vibration. The soil domain area A is selected by evaluating the building base to bedrock transfer function (TF) that is the ratio of the Fourier spectrum of acceleration signals at the building base and soil-bedrock interface. The frequency corresponding to the peak of this TF matches the soil column fundamental frequency in the FF case, when the soil domain area A is wide, and it is progressively lower with a decreasing soil area. The selected soil domain area is the smallest for which the peak of the building base to bedrock TF corresponds to a soil column fundamental frequency equivalent to the FF case. In this research, a squared soil area is used, after evaluation of the building base to bedrock TF for both horizontal directions of motion and verification that the adopted dimension is convenient for both directions.

The building top to bottom TF, that provides the fixed-base natural frequency of the building, is not influenced by the variation of the soil domain area. The building top to bedrock TF gives the frequency of the building-soil system. All the TF are evaluated in a linear elastic regime.

3. 1DT-3C WAVE PROPAGATION MODEL FOR SSI AND SSSI ANALYSES

A 3D soil model permits taking into account the spatial variability of soil properties, topography effects, foundation deformability, rocking effects and the presence of a group of buildings at the soil surface. Lateral absorbing conditions are necessary as lateral boundaries when the spatial variability of soil properties and topography effects are modeled, since the periodic lateral boundary condition is no more verified because different strain conditions at the left and right side of the soil domain surface waves are induced and surface waves appear.

The 1D-3C wave propagation approach for SSI investigations (Fig. 1a), discussed in Section 2, is limited to the case of rigid shallow foundation, negligible rocking effects, horizontally layered soil with periodic lateral boundary condition and homogeneous properties in each layer. Furthermore, the numerical simulation of seismic response of a group of buildings can only be solved in a fully 3D soil domain. In this research, a modeling technique is proposed to take into account the foundation deformability, rocking effects and the cross-interaction between neighbor structures and the soil. It is inspired by the consideration that SSI and SSSI are detected in the near-surface soil layers. A fully 3D soil model is adopted until a fixed depth h and a 1D model is used for deeper soil layers (Fig. 4). Due to the T-shaped soil domain, the proposed modeling technique is named as 1DT-3C wave propagation approach for SSI and SSSI analyses (Fig. 5).

A constraint equation is used to condense out the degrees of freedom at the base of the 3D soil domain to those at the top of the unit area soil column.

The foundation is modeled using 20-node solid FE and it is embedded in the soil domain. Consequently, the foundation deformability and its rigid rotation, due to rocking effects, can be taken into account and the seismic motion at the base of each building column is independent.

In this research, the periodic lateral boundary condition is maintained at the lateral boundaries all along the depth. When the periodicity is not assured, an absorbing condition could be imposed at the lateral boundaries of the 3D soil domain, until the fixed depth h (Fig. 4).

The proposed 1DT-3C wave propagation approach for SSI analyses is not dependent on the constitutive model adopted for soil and structure.

The proposed 1DT-3C wave propagation model, compared with a fully 3D model, still reduces the modeling time because the boundary condition definition is simple, especially in the case of periodic lateral boundary condition, because the input motion and the absorbing condition are defined in only one element at the base. Moreover, a one-dimensional soil profile can be characterized with a single borehole investigation, instead a 3D soil domain needs more investigations to define in a reliable way the geotechnical model.

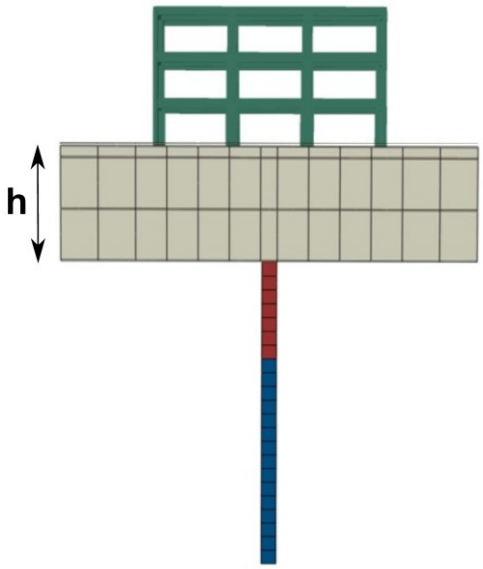

Fig. 4. 1DT-3C wave propagation model for soil-structure interaction analysis, where a fully 3D soil model is adopted until a fixed depth h and a 1D model is used for deeper soil layers.

3.1. Soil depth concerned by the SSI

The depth of the fully 3D soil domain is fixed after analysis of the results obtained using the 1D-3C wave propagation model (Fig. 1a) in a linear elastic regime, compared with a simulation in FF conditions. The effect of SSI is not negligible where the maximum shear strain profiles with depth are remarkably different. Hence, in the 1DT soil model (Fig. 4), a 3D soil domain is assumed until a depth h, where the SSI is present, and a 1D model is used in deeper soil layers.

As the 1D-3C wave propagation model (Fig. 1a) considers only the inertial SSI, but does not consider the rocking effect and the foundation deformability, it can be convenient to check the adopted assumption of the height h to be sure that with a slightly deeper 3D soil domain the results are not significantly different in terms of displacement and acceleration time history.

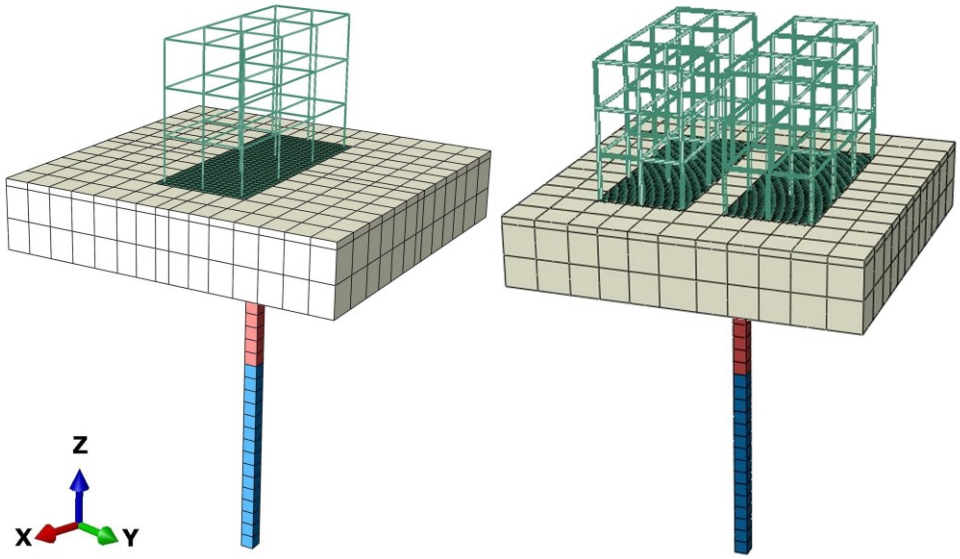

Fig. 5. 1DT-3C model for soil-structure interaction (left) and for structure-soil-structure (right) analysis.

4. VERIFICATION OF THE PROPOSED MODELS

The 1D-3C and 1DT-3C wave propagation models are verified by comparison with the case of 3D soil domain and embedded foundation, for vertical propagation, horizontally layered soil having nonlinear behavior and periodic lateral boundary condition.

The 1DT-3C and 3D-3C wave propagation models take into account the foundation deformability, rocking effects and the cross-interaction between neighbor structures and the soil.

Anderson's criteria [19] are employed to quantitatively estimate the reliability of results obtained using the proposed models, compared with the reference numerical model. The Goodness-of-fit (Gof) is represented using grades between 0 and 10, assigned to ten parameters characterizing a signal: Arias duration (C1), energy duration (C2), Arias intensity (C3), energy integral (C4), peak acceleration (C5), velocity (C6) and displacement (C7), response spectrum (C8), Fourier spectrum (C9) and cross correlation ratio (C10). Scores in the intervals 0-4, 4-6, 6-8 and 8-10 represent poor, fair, good and excellent fit, respectively.

4.1. Soil and building data

The stratigraphy and mechanical parameters of soil profiles used in the verification phase are identified in Table 1. Soil properties are assumed homogeneous in each soil layer. The soil density ρ and the shear and compressional wave velocities in the medium v_s and v_p, respectively, allow the computation of the elastic shear and P-wave moduli $G_0 = \rho v_s^2$ and $M_0 = \rho v_p^2$. The shear wave velocity profile is arbitrary fixed. Densities and compressional wave velocities are deduced according to the relationships discussed by Boore [20]. The Poisson's ratio $\nu = \left(0.5 v_p^2 / v_s^2 - 1\right) \Big/ \left(v_p^2 / v_s^2 - 1\right)$ is evaluated as function of the compressional to shear velocity ratio. The reference shear strain is assumed equal to $\gamma_r = 0.35‰$ for all layers.

In the soil domain, the mesh size is one quadratic solid element every meter in the 1D column having unit area and one element every two meters in the 3D domain.

The two three-story buildings which floor plans are shown in Fig. 6 are used for the following analyses. The choice of a limited number of spans is motivated by the fact that an increasing number of spans does not modify the natural frequencies associated to the first mode shapes, implying an increase of both mass and stiffness but a constant stiffness to mass ratio.

Table 1

Stratigraphy and mechanical features of the analyzed multilayered soil profiles having different fundamental frequency f_s.

	Profile f_s = 3.8 Hz			Profile f_s = 1.9 Hz		
Depth (m)	density (kg/m^3)	S-wave velocity (m/s)	P-wave velocity (m/s)	density (kg/m^3)	S-wave velocity (m/s)	P-wave velocity (m/s)
0-5	1930	250	1417	1930	180	1293
5-15	1947	340	1568	1930	200	1329
15-30	2019	500	1815	1930	240	1400
> 30	2100	1000	2449	2100	1000	2449

Consequently, it is not useful, for the scope of the presented analysis, to increase the modeling and computation time. The number of stories is determined according to the desired fundamental frequency of the building, for the purpose of the analysis.

The building in Fig. 6a has the same inertia to horizontal motion in the two orthogonal directions x and y due to column orientation, despite the rectangular floor plan. Its first and second natural frequencies are equal to $f_b = 3.8\,\text{Hz}$. The building in Fig. 6b has very different inertia to horizontal displacement in the two orthogonal directions x and y, consequently, the first two natural frequencies are distinct. The first natural frequency is equal to $f_{b1} = 2.8\,\text{Hz}$ and

corresponds to a translational mode shape in x-direction, while the second one is $f_{b2} = 4.7\,\mathrm{Hz}$ and is related to a translational mode shape in y-direction. Building dimensions are indicated in Fig. 6. The interstory height is 3.2 m. The rectangular cross-section of beams at the first and second floor has dimensions $0.3m \times 0.7m$ and that of beams at the third floor has dimensions $0.3m \times 0.6m$. The cross-section of columns is $0.3m \times 0.8m$, $0.3m \times 0.7m$ and $0.3m \times 0.6m$ for the first, second and third floor, respectively. A live and dead load of $700\,\mathrm{Kg/m^2}$ is distributed on beams in x-direction, according to their influence area, as mass per unit length. Mechanical properties of concrete are the elastic modulus in compression $E = 31220 \times 10^6\,\mathrm{N/m^2}$ and the Poisson's ratio $\nu = 0.2$ (shear correction factor $\chi = 0.857$). The reinforced concrete density is $\rho = 2500\,\mathrm{kg/m^3}$ and the damping ratio is $\zeta = 5\%$.

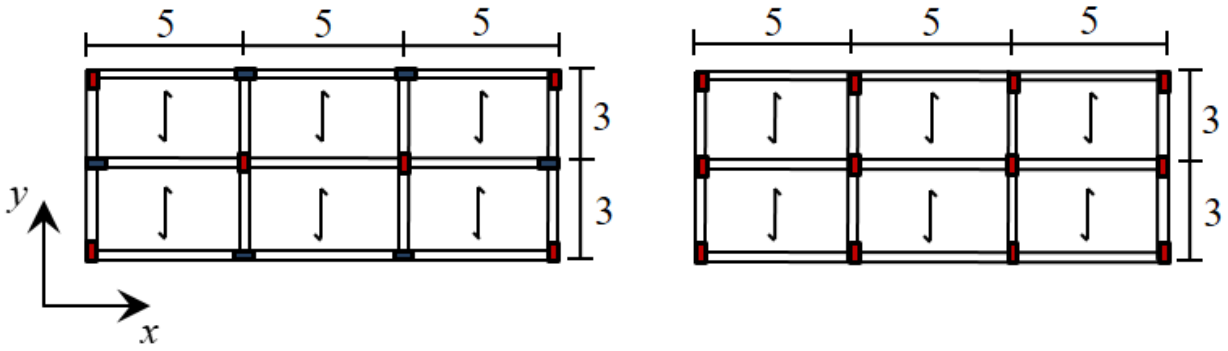

(a) (b)

Fig. 6. Floor plan of the two analyzed three-story buildings that have same (a) and different (b) inertia to horizontal motion in the two orthogonal directions *x* and *y*. The dimensions of the two buildings are the same; the difference is in the rectangular column orientation.

Fig. 7 shows the building bottom to bedrock TF for the soil profile and building having fundamental frequency $f_s = f_b = 3.8\,\mathrm{Hz}$ (Table 1 and Fig. 6a), for different soil areas, obtained

using a 1D-3C wave propagation model as explained in Section 2.5. A squared soil area $A = 25\,\mathrm{m} \times 25\,\mathrm{m}$ is selected for the following analyses, knowing that the building is $15\,\mathrm{m}$ long.

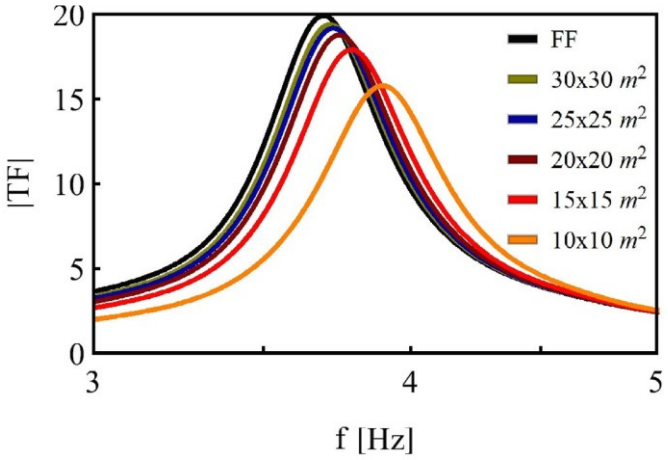

Fig. 7. Building base to bedrock Transfer Function, evaluated for different soil areas, and free-field to bedrock Transfer Function (FF).

4.2. Input motion

A recorded signal of the 6 April 2009 Mw 6.3 L'Aquila earthquake is used as rock outcropping motion for the verification phase. The signal is recorded at the Antrodoco (ANT) station of the Italian strong motion network, localized in Lazio region (Italy), at an epicentral distance of 26.2 km. The ANT is a FF station in a flat surface (slope angle lower than 15°) and on a stiff soil (type A in the Eurocode 8 soil classification). The PGA is $0.2597\,\mathrm{m/s^2}$, observed in North-South (NS) direction. The ground acceleration is $0.1974\,\mathrm{m/s^2}$ and $0.1147\,\mathrm{m/s^2}$ in East-West (EW) and Up-Down (UP) direction, respectively. According to the Fourier spectrum of the NS component (Fig. 8b), the frequency associated to the highest-energy content is $1.9\,\mathrm{Hz}$. The sample rate of the recorded signals is $dt = 5 \times 10^{-3}\,\mathrm{s}$.

The selected seismic signal is applied at the base of the horizontally multilayered soil profile in

terms of velocity (Fig. 8a).

All numerical signals in the present analysis are filtered by a zero-phase-shift two pole Butterworth filter between 0.1 and 10 Hz, that is a band including the most relevant frequency content of the building.

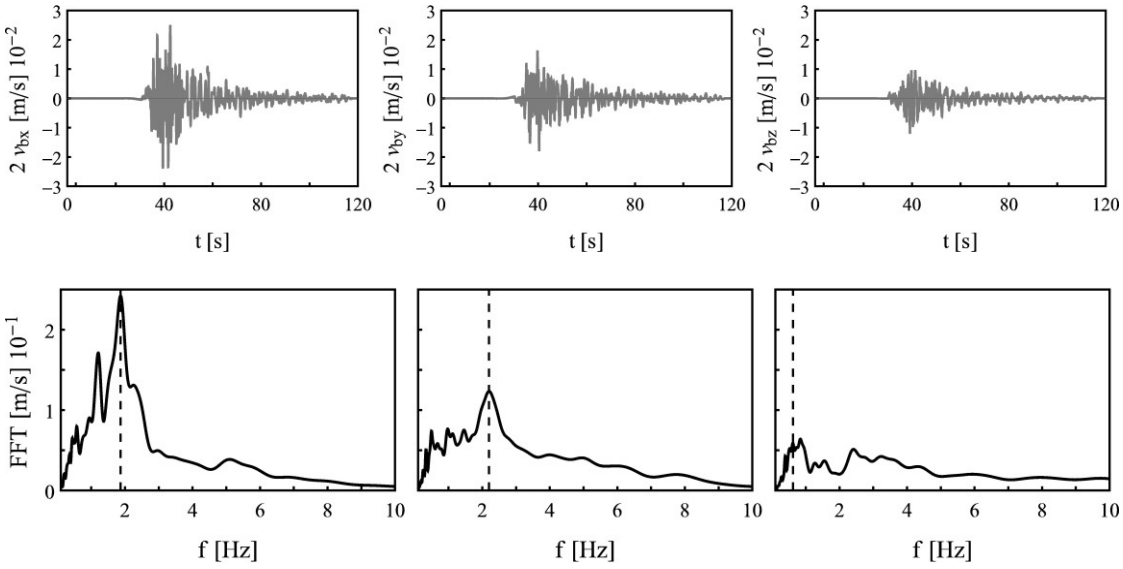

Fig. 8. Velocity time history (top) and Fourier spectrum (bottom) for the NS, EW and UP components of the 2009 Mw 6.3 L'Aquila earthquake at recorded ANT station. Dashed lines show the predominant frequency in NS, EW and UP directions.

4.3. Verification

The 1D-3C wave propagation model for SSI analysis (Fig. 1a) is compared with a 3D-3C soil-foundation-structure interaction model where the reinforced concrete foundation is modeled as embedded in the soil domain (Fig. 1c), under the assumption of periodic lateral boundary condition and vertical propagation along a horizontally layered soil. The 3D-3C model is able to take into account the foundation deformability and rocking effects.

The three-story building in Fig. 6a (same inertia in both orthogonal directions, $f_b = 3.8\,\mathrm{Hz}$) is

associated with the soil profile having $f_s = 3.8\,\mathrm{Hz}$ and nonlinear behavior. The rigid foundation, embedded in the soil, is 16 m long by 7 m wide and 0.5 m deep. The concrete properties are the same for the foundation and the structure.

The GoF criteria are listed in Table 2. An excellent fit is obtained for all comparisons, in the case of resonance (building and soil fundamental frequency close together). The acceleration and roof drift time histories at the building bottom and top, respectively, obtained using the 1D-3C and 3D-3C wave propagation models are shown in Fig. 9. According to the results presented in Table 2 and Fig. 9, the differences between the two models in Fig. 1a and 1c are negligible, when the foundation deformability and rocking effects are reduced.

In this computation (Table 2), the dynamic equilibrium equation for the soil-structure assembly is solved in $10\,\mathrm{m}57\,\mathrm{s}$ using the 1D-3C model (Fig. 1a) and in $2\,\mathrm{h}16\,\mathrm{m}54\,\mathrm{s}$ using the 3D-3C model (Fig. 1c), for a three-component input motion of $120\,\mathrm{s}$ and nonlinear behaving soil, using 1 core and 24 nodes (see Data and Resources section).

Table 2

Goodness-of-fit of 1D-3C and 1DT-3C wave propagation approaches, with respect to a 3D-3C seismic wave propagation model.

Compared models		Position	Direction	Anderson criteria									
				C1	C2	C3	C4	C5	C6	C7	C8	C9	C10
1D-3C	3D-3C	bldg. base	X	10	10	10	10	10	10	10	10	9.9	10
			Y	10	10	10	10	10	10	10	10	9.8	10
			Z	9.8	10	10	10	10	10	10	10	8.7	9.6
1D-3C	3D-3C	bldg. top	X	9.4	9.6	10	10	9.9	10	10	10	9.7	9.4
			Y	9.7	9.8	10	10	10	10	10	10	9.7	9.9
			Z	9.6	9.9	9.7	10	10	10	10	10	8.8	9.7
1DT-3C	3D-3C	bldg. base	X	10	10	10	10	10	10	10	10	9.5	10
			Y	10	10	10	10	10	10	10	10	9.3	10
			Z	9.7	10	9.9	10	10	10	10	10	8.4	9.9

1DT-3C	3D-3C	bldg. top	X	9.9	9.9	10	10	10	10	10	10	9.3	10
			Y	9.9	10	10	10	10	10	10	10	9.0	10
			Z	9.7	10	9.9	10	10	10	10	10	8.5	9.9

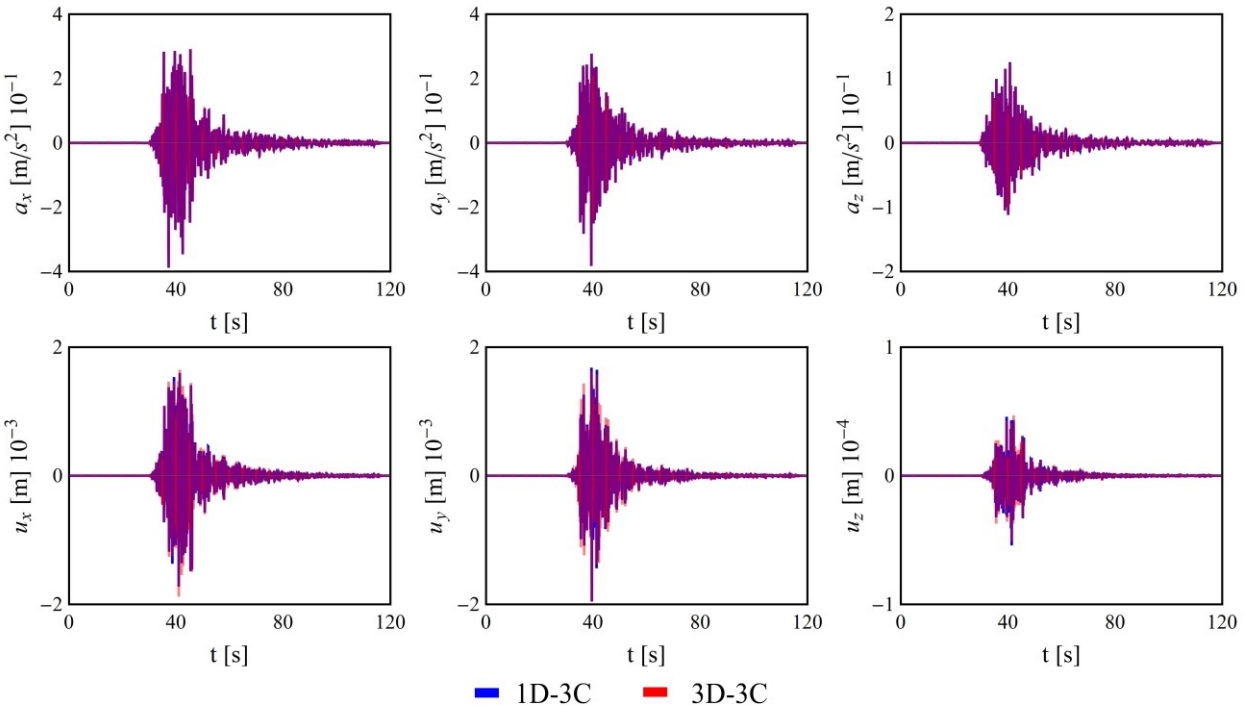

Fig. 9. Comparison of 1D-3C and 3D-3C wave propagation approaches for SSI analysis: acceleration time history at the building bottom (top) and roof drift time history at the building top (bottom).

The 1DT-3C wave propagation model and the 3D-3C model with the reinforced concrete foundation, shown in Fig. 1a and 1c respectively, are compared for the same case of building having $f_b = 3.8\,\text{Hz}$ (Fig. 6a), placed on the soil profile having $f_s = 3.8\,\text{Hz}$ and nonlinear behavior. The depth of the fully 3D soil domain is fixed comparing the results obtained using the 1D-3C wave propagation model (1D all along the soil column), in a linear elastic regime, with a simulation in FF conditions. Results of the maximum shear strain and stress profiles with depth are shown in Fig. 10. Only in the first meters the effect of SSI is not negligible. Hence, in the

1DT soil model (Fig. 4), a 3D soil domain is assumed until a depth $h = 5\,\mathrm{m}$, that corresponds to the interface between the first and second soil layers, and a 1D model is used in deeper soil layers.

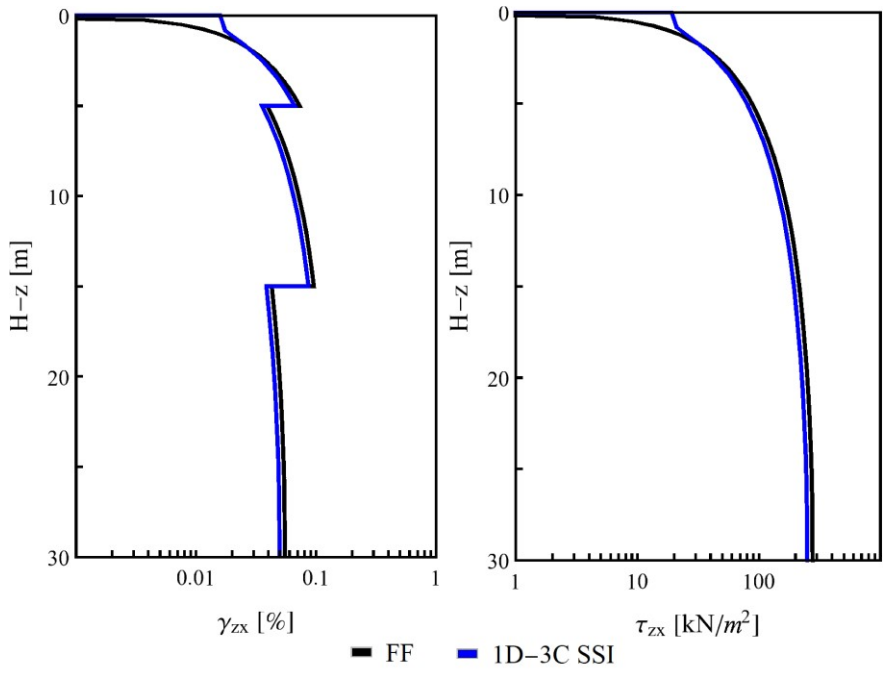

Fig. 10. Maximum shear strain (left) and stress (right) profile with depth obtained using de 1D-3C wave propagation model for the SSI analysis in a linear elastic regime.

GoF show excellent fit of the 1DT-3C wave propagation approach compared with a 3D-3C model, as reported in Table 2. The acceleration and roof drift time histories at the building bottom and top, respectively, are shown in Fig. 11. The energy integral, the pseudo-acceleration response spectrum and Fourier spectrum in direction *x* are represented in Fig. 12 to confirm the excellent fit given by the GoF scores (C4, C8 and C9, respectively, in Table 2). The correlation of the estimated acceleration in *x* direction is shown in Fig. 13.

These comparisons with respect to the case of a 3D soil domain allow the verification of the 1DT-3C wave propagation approach, in the case of periodic lateral boundary condition and

vertical propagation along a horizontally layered soil. Moreover, it is checked that the selected thickness h of the 3D soil layer is suitable for this particular stratigraphy.

In this computation (Table 2), the dynamic equilibrium equation for the soil-structure assembly is solved in $1\,\mathrm{h}\,20\,\mathrm{m}\,7\,\mathrm{s}$ using the 1DT-3C model (Fig. 5a) and in $2\,\mathrm{h}\,16\,\mathrm{m}\,54\,\mathrm{s}$ using the 3D-3C model (Fig. 1c), for a three-component input motion of $120\,\mathrm{s}$ and nonlinear behaving soil, using 1 core and 24 nodes (see Data and Resources section).

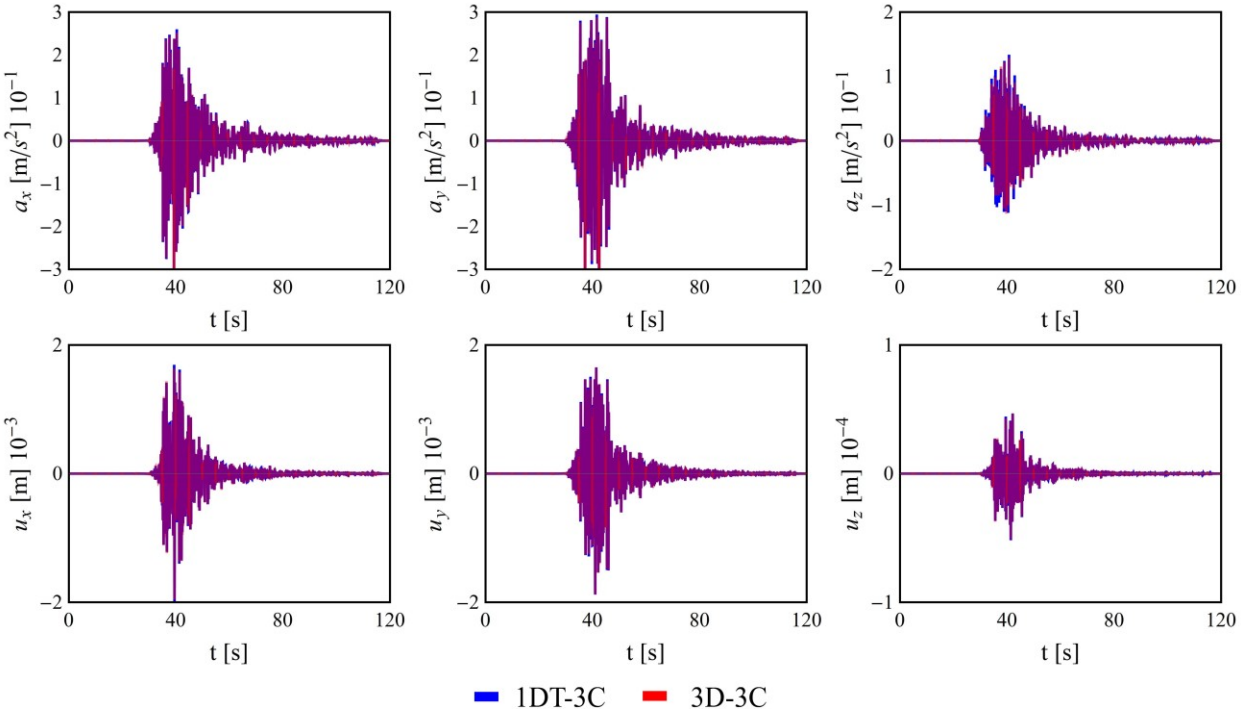

Fig. 11. Comparison of 1DT-3C and 3D-3C wave propagation approaches for SSI analysis: acceleration time history at the building bottom (top) and roof drift time history at the building top (bottom).

5. SSI ANALYSIS

A synthetic wavelet has been used as seismic loading in the following analyses, in order to use a narrow-band input motion whose predominant frequency can be imposed in such a way to be

close to a selected natural frequency of the building-soil system.

The seismic loading is applied in terms of velocity (Mavroeidis and Papageorgiou [21]) and has the following expression:

$$v_0(t) = v_{0\max}/2\left[1+\cos\left(2\pi f_q/n\left(t-t_0\right)\right)\right]\cos\left(2\pi f_q\left(t-t_0\right)\right) \quad (1)$$

The motion duration is $2t_0$, where $t_0 = n/(2f_q)$ is the time of envelope peak, the predominant frequency is f_q and $n=5$ is the number of cycles. The peak acceleration at the soil-bedrock interface in North-South, East-West and Up-Down directions is imposed as $a_{0\max} = 1.75\,\mathrm{m/s^2}$.

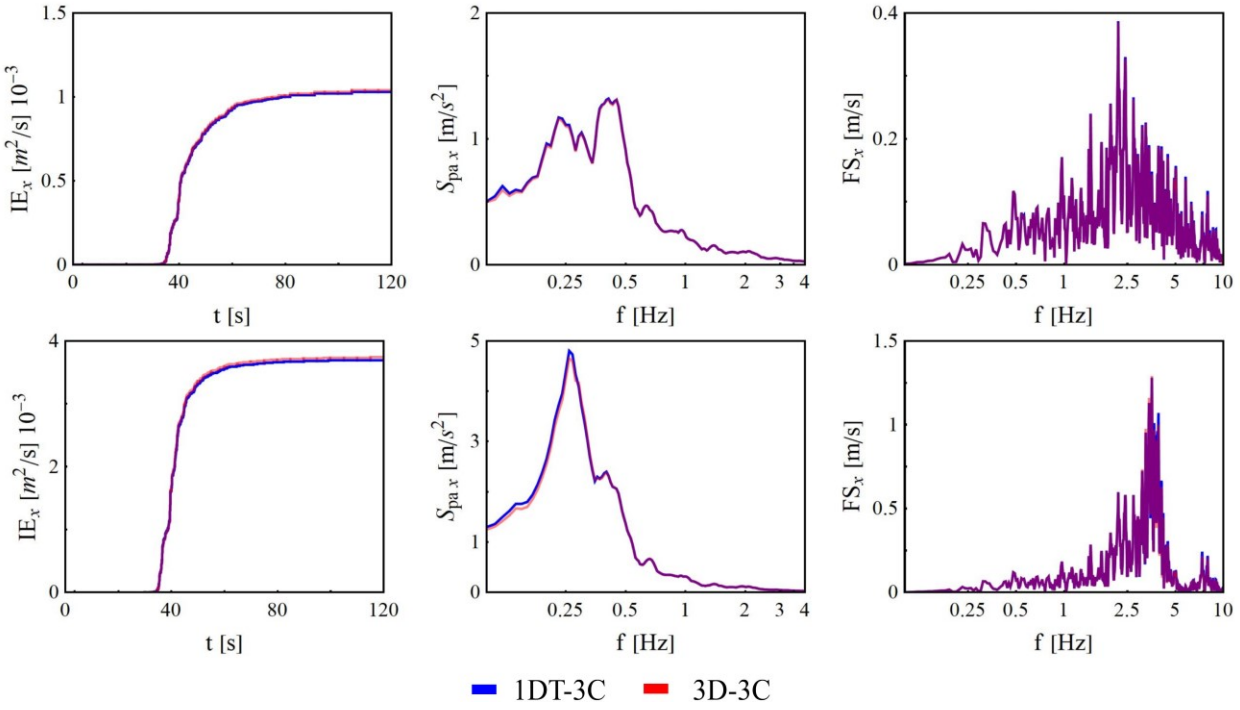

Fig. 12. Comparison of 1DT-3C and 3D-3C wave propagation approaches for SSI analysis: energy integral (IE), response spectrum acceleration (S_{pa}) and Fourier spectrum (FS) for the horizontal *x*-component of motion at the building bottom (top) and top (bottom).

5.1 Impact of the excitation frequency on the structural response

The 1DT-3C wave propagation approach for SSI analysis is used in order to understand the impact of the seismic motion frequency content on the response of a building over a horizontally layered soil.

The building-soil system composed by a T-shaped soil profile having natural frequency $f_s = 1.9\,\text{Hz}$ (Table 1) and a building having fundamental frequency $f_b = 3.8\,\text{Hz}$ (Fig. 6a) is first shaken by a seismic loading (Eq (1)) having predominant frequency $f_q = f_b = 3.8\,\text{Hz}$, close to the fixed-base building frequency, and then by another having $f_q = f_s = 1.9\,\text{Hz}$, close to the soil column frequency.

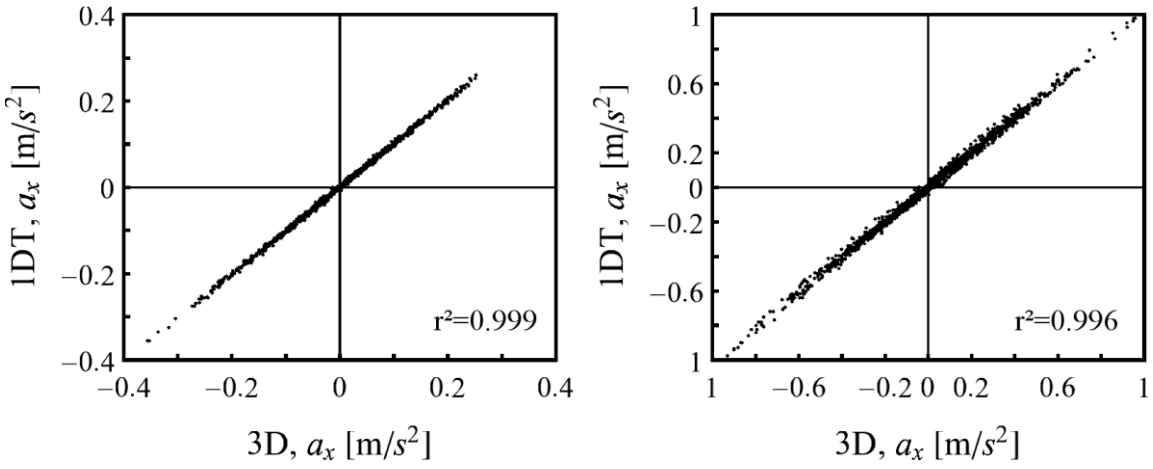

(a) (b)

Fig. 13. Comparison of 1DT-3C and 3D-3C wave propagation approaches for SSI analysis: correlation coefficient of accelerations for the horizontal *x*-component of motion at the building bottom (a) and top (b).

Fig. 14 shows an amplification of the acceleration at the building bottom in the case where the soil frequency is excited $\left(f_q = f_s = 1.9\,\text{Hz}\right)$, that implies an amplification of the seismic loading for the building. However, the higher roof drift at the building top (Fig. 14) is obtained for the

case where the predominant frequency of the earthquake is close to the fixed-base frequency of the building $\left(f_q = f_b = 3.8\,\text{Hz}\right)$. This result signifies that the frequency content of the seismic load imposed at the bottom of the building is more important for the building deformation than the concept of expected maximum ground acceleration amplitude, derived from building design in static conditions.

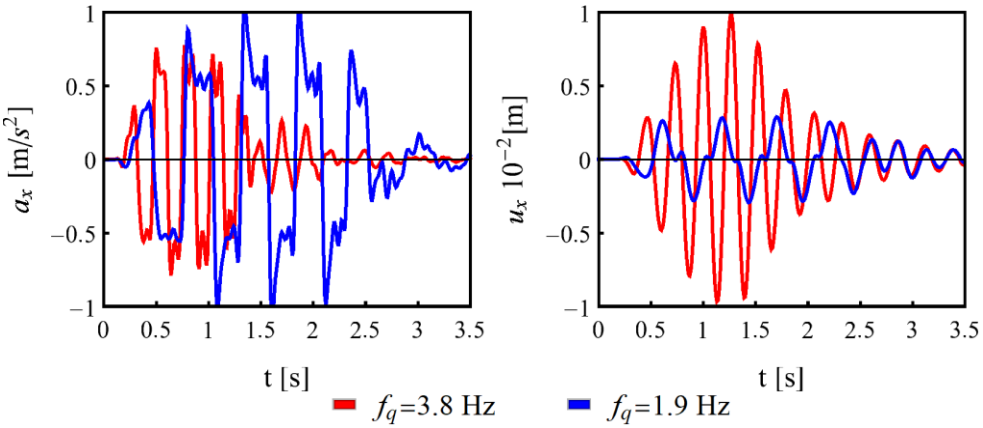

Fig. 14 Acceleration time history at the building bottom (left) and roof drift at the building top (right), for the building-soil system composed by a T-shaped horizontally layered soil having frequency $f_s = 1.9\,\text{Hz}$ and a building having fundamental frequency $f_b = 3.8\,\text{Hz}$, in the case of earthquake predominant frequency equal to $f_q = f_b = 3.8\,\text{Hz}$ and $f_q = f_s = 1.9\,\text{Hz}$.

Furthermore, Fig. 15 shows the building top to bottom TF in the cases of fixed-base building and SSI analysis, using the 1DT-3C wave propagation approach, for the two cases of soil profile having $f_s = f_b = 3.8\,\text{Hz}$ and $f_s = 1.9\,\text{Hz} < f_b = 3.8\,\text{Hz}$. It can be observed a reduction of the building fundamental frequency due to SSI, that is $f_{SSI} = 3.6\,\text{Hz}$. In this case of three-story building, the variation of frequency, also for softer soil $\left(f_s = 1.9\,\text{Hz}\right)$, is not important because rocking effects are reduced. It is expected that more important rocking effects would reduce the

building frequency when SSI is considered.

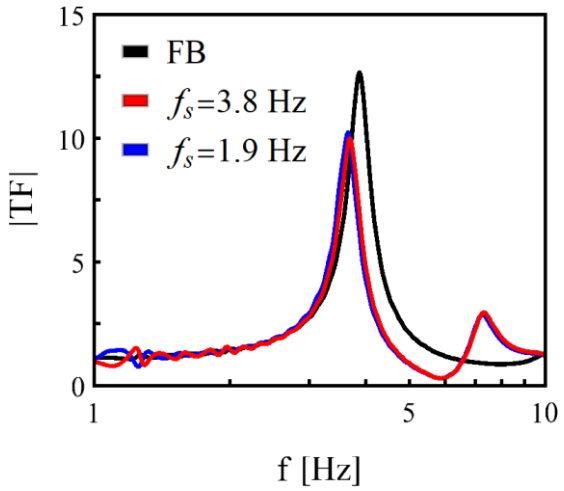

Fig. 15. Building top to bottom transfer function estimated for a fixed-base building and for SSI analysis in the cases of building-soil resonance $\left(f_s = f_b = 3.8\,\text{Hz}\right)$ and softer soil $\left(f_s = 1.9\,\text{Hz} < f_b = 3.8\,\text{Hz}\right)$.

5.2 SSI estimation

The 1DT-3C seismic wave propagation model is used to compare the seismic response of a building-soil system shaken by a seismic loading (Eq (1)) having predominant frequency f_q equal to the fundamental frequency of the building, f_b. The analysis is done in both cases of horizontally layered soil having natural frequency $f_s = f_b$ and $f_s < f_b$.

The building having $f_b = 3.8\,\text{Hz}$ (Fig. 6a) is placed at the surface of the soil profiles having $f_s = 3.8\,\text{Hz}$ and $f_s = 1.9\,\text{Hz}$. The input seismic signal has predominant frequency $f_q = f_b = 3.8\,\text{Hz}$. The acceleration time history at the building bottom and the roof drift at the building top are shown in Fig. 16 for the cases of one-step analysis (building-soil system) and

two-step analysis (FF motion at the base of a FB building). Taking into account the SSI, using a one-step analysis, gives a reduction of structural deformation.

The SSI effect is quantitatively measured as the one-step to two-step ratio of the maximum acceleration at the building top, $a_{\max\_1step}/a_{\max\_2step}$. It is obtained $a_{\max\_1step}/a_{\max\_2step} = 0.69$ and $a_{\max\_1step}/a_{\max\_2step} = 0.57$, for both x- and y-direction, in the cases $f_s = f_b = f_q = 3.8\,\text{Hz}$ and $f_s = 1.9\text{Hz} < f_b = f_q = 3.8\,\text{Hz}$ respectively. The SSI is more important in the case where the soil is softer (lower $a_{\max\_1step}/a_{\max\_2step}$ ratio), in the case of nonlinear soil behavior. The resonance effect $\left(f_s = f_b = f_q = 3.8\,\text{Hz}\right)$ produces an amplified seismic response, as can be observed by comparing Fig. 16a and 16b.

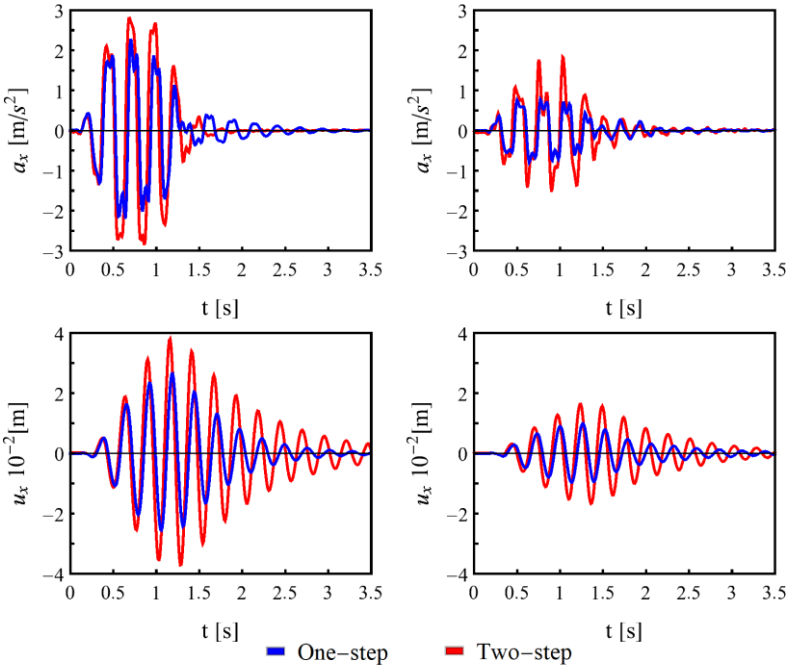

(a) (b)

Fig. 16. Acceleration time history at the building bottom and roof drift at the building top, for the building-soil system composed by a building having fundamental frequency $f_b = 3.8\,\text{Hz}$ and a

T-shaped horizontally layered soil having frequency $f_s = f_b = 3.8\,\text{Hz}$ (a) and $f_s = 1.9\,\text{Hz} < f_b = 3.8\,\text{Hz}$ (b), in the case of earthquake predominant frequency equal to $f_q = f_b = 3.8\,\text{Hz}$.

5.3 1st vs 2nd natural frequency

The building represented in Fig. 6b, having natural frequencies $f_{b1} = 2.8\,\text{Hz}$ and $f_{b2} = 4.7\text{Hz}$, is placed at the surface of the soil profile having natural frequency $f_s = 1.9\,\text{Hz}$. Fig. 17 and 18 show the comparison between the results obtained by a one-step analysis, using the 1DT-3C wave propagation approach, and a two-step analysis, in terms of acceleration at the building bottom and the roof drift at the building top. In particular, the cases of input seismic loading (Eq (1)) having predominant frequency equal to the first $\left(f_q = f_{b1} = 2.8\,\text{Hz}\right)$ and second $\left(f_q = f_{b2} = 4.7\,\text{Hz}\right)$ natural frequency of the building are shown in Fig. 17 and 18, respectively.

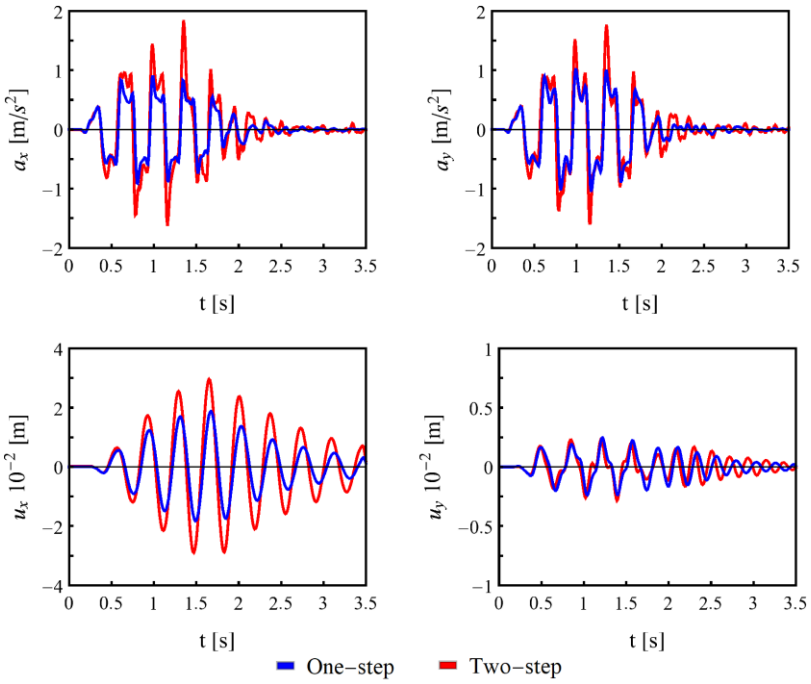

Fig. 17. Acceleration time history at the building bottom and roof drift at the building top, for the building-soil system composed by a building having fundamental frequencies $f_{b1} = 2.8\,\text{Hz}$ and $f_{b2} = 4.7\,\text{Hz}$ and a T-shaped horizontally layered soil having frequency $f_s = 1.9\,\text{Hz}$, in the case of earthquake predominant frequency equal to $f_q = f_{b1} = 2.8\,\text{Hz}$.

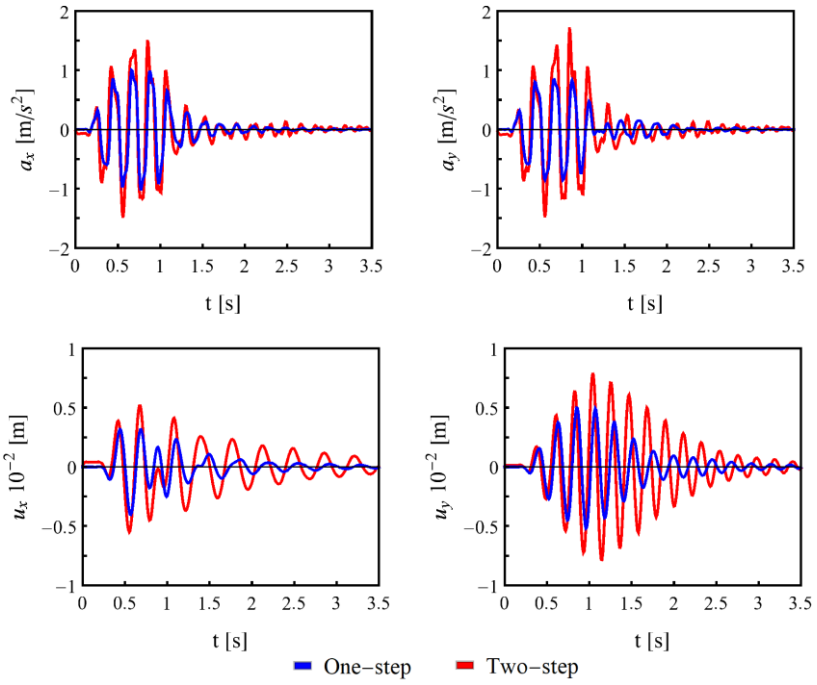

Fig. 18. Acceleration time history at the building bottom and roof drift at the building top, for the building-soil system composed by a building having fundamental frequencies $f_{b1} = 2.8\,\text{Hz}$ and $f_{b2} = 4.7\,\text{Hz}$ and a T-shaped horizontally layered soil having frequency $f_s = 1.9\,\text{Hz}$, in the case of earthquake predominant frequency equal to $f_q = f_{b2} = 4.7\text{Hz}$.

The one-step to two-step ratio of the maximum acceleration at the building top, quantitatively estimating the SSI effect, is $a_{\max\_1step}/a_{\max\_2step} = 0.58$ for x-direction and $a_{\max\_1step}/a_{\max\_2step} = 0.71$ for y-direction, in the case where $f_q = f_{b1} = 2.8\,\text{Hz}$ and

$a_{\max\_1step}/a_{\max\_2step} = 0.65$ for x-direction and $a_{\max\_1step}/a_{\max\_2step} = 0.56$ for y-direction, in the case where $f_q = f_{b2} = 4.7\,\text{Hz}$. SSI effect in the soil is obtained for both directions. SSI effect is more pronounced, in the structure, in the direction of the building mode shape excited by the input load.

6. CONCLUSIONS

A first part of this research proposes a modeling technique for structural design that can be applied using common finite element codes, where soil-structure interaction (SSI) and seismic site effects are taken into account adopting a one-directional three-component (1D-3C) seismic wave propagation model.

The dynamic equilibrium problem is directly solved for a building-soil assembly, composed of a three-dimensional frame structure and a multilayered soil column modeled using unit area solid FE, in the case of rigid shallow foundation, vertical propagation and periodic condition at the lateral boundaries. Compared with a detailed 3D soil model, the geotechnical characterization of a soil column is more adapted to the engineering practice, needing a single borehole investigation. Moreover, the proposed model strongly reduces the computational time.

The 1D-3C wave propagation approach for SSI is verified by comparison with a fully 3D model, in the case of vertical propagation in a horizontally layered soil having nonlinear behavior. Nevertheless, the hypothesis of rigid shallow foundation, with the same seismic motion at the base of all columns, does not permit to consider the foundation deformability and rocking effects and this model cannot simulate the interaction between more buildings.

A 1DT-3C seismic wave propagation model is proposed as modeling technique for the simulation of the response of soil and building to earthquakes, taking into account site effects,

the foundation deformability, rocking effects and structure-soil-structure interaction. A fully 3D model is adopted until a fixed depth, where SSI and SSSI effects are considered to modify the ground motion, and for deeper layers a 1D model is used and supposed a sufficient approximation.

The 1DT-3C wave propagation approach is verified by comparison with a fully 3D-3C model, in the case of vertical propagation in a horizontally layered soil. The proposed 1DT-3C wave propagation modeling technique is an efficient tool for building design allowing SSI to be taken into account in an effective and easy way. In fact, in the case of vertical propagation and homogeneous geotechnical parameters in each soil layer, using unit area solid elements for deeper layers, instead of a 3D domain, represents a reduction of computational time without affecting the results.

The use of the 1DT-3C wave propagation approach for SSI analyses shows that the frequency content of the seismic load imposed at the bottom of the building can be more significant for the building deformation than the concept of expected maximum ground acceleration amplitude, derived from building design in static conditions.

The SSI effect is defined as difference between the direct solution of the dynamic equilibrium problem of the assembly of soil and building (one-step solution) and the free-field motion applied to a fixed-base building (two-step analysis), in terms of maximum acceleration ratio $a_{\max\_1step}/a_{\max\_2step}$. It appears more important in the case where the soil is softer, when the soil behavior is nonlinear. The resonance between building, soil and earthquake frequency content produces an amplified seismic response.

SSI effect is observed for both translational mode shapes and it is more pronounced, for the structural behavior, in the direction of the mode shape excited by the input load.

Further studies will be undertaken using the 1DT-3C wave propagation approach for structure-soil-structure interaction analyses to understand the effect on structural seismic response of an adjacent building.

DATA AND RESOURCES

This research is performed using HPC resources from GENCI-[CINES] (Grant 2017-[A0010410071]).

Seismograms used in this study are provided by the Instituto Nazionale di Geofisica e Vulcanologia (INGV) in Italy and can be obtained from Itaca database (Italian Accelerometric Archive) at http://itaca.mi.ingv.it (last accessed June 2017).

ACKNOWLEDGMENTS

This work has been funded by the region Provence-Alpes-Côte d'Azur (South-Eastern France) through a doctoral fellowship. The authors thank the Fédération W. Döblin for financial support and promotion of inter-laboratory collaboration. This work benefits from scientific discussions with Fernando Lopez Caballero (Centrale-Supélec, France) and the authors deeply thank him for his advice and support.

REFERENCES

[1] European Committee for Standardisation, EN 1998-5: Eurocode 8: Design of structures for earthquake resistance - Part 5: Foundations, retaining structures and geotechnical aspects 2003.

[2] Saez E, Lopez Caballero F, Modaressi-Farahmand-Razavi A. Effect of the inelastic

dynamic soil–structure interaction on the seismic vulnerability assessment. Struct. Safety 2011; 33(1):51–63.

[3] Mylonakis G, Gazetas G. Seismic soil-structure interaction: beneficial or detrimental?. J. Earthq. Eng. 2000; 4(3):277–301.

[4] Stewart JP, Fenves GL, Seed RB. Seismic Soil-Structure Interaction in Buildings. II: Empirical Findings. J. Geotech. Geoenviron. Eng. 1999; 125(1):38–48.

[5] Jennings PC, Bielak J. Dynamics of building-soil interaction. Bull. Seism. Soc. Am. 1973; 63(1):9–48.

[6] Jeremic B, Tafazzoli N, Kamrani B, Tasiopoulou P, Jeong CG. Investigation of Analysis Methods to Incorporate Multi-Dimensional Loading and Incoherent Ground Motions in Soil-Structure Interaction Analysis. Report to the US Nuclear Regulatory Commission (NRC) 2011.

[7] Coleman J, Whittaker A, Jeremic B. Nonlinear Time Domain Seismic Soil Structure Interaction (SSI) Analysis for Nuclear Facilities and Draft Appendix B of ASCE 4. Proc. of the Structural Mechanics in Reactor Technology, San Francisco 2013.

[8] Santisi d'Avila MP, Lopez Caballero F. Analysis of nonlinear Soil-Structure Interaction effects: 3D frame structure and 1-Directional propagation of a 3-Component seismic wave. Comput. Struct. 2018, in press.

[9] Zienkiewicz OC, Bicanic N, Shen FQ. Earthquake input definition and the transmitting boundary conditions. Adv. Comput. Linear Mech., Springer Vienna, 1988; 300:109–138.

[10] Joyner WB, Chen ATF. Calculation of nonlinear ground response in earthquakes. Bull. Seism. Soc. Am. 1975; 65:1315–36.

[11] Iwan WD. On a Class of Models for the Yielding Behavior of Continuous and Composite Systems. J. Appl. Mech. 1967; 34:612–7.

[12] Joyner WB. A method for calculating nonlinear seismic response in two dimensions. Bull. Seism. Soc. Am. 1975; 65:1337–57.

[13] Kramer SL. Geotechnical earthquake engineering. Prentice Hall, New York 1996.

[14] Hardin BO, Drnevich VP. Shear modulus and damping in soils: design equations and curves. ASCE J. Soil Mech. Found. Div. 1972; 98(7):667-692.

[15] Santisi d'Avila MP, Semblat JF, Lenti L. Modeling strong seismic ground motion: 3D loading path vs wavefield polarization. Geophys. J. Int. 2012; 190:1607–1624.

[16] Kaneko T. On Timoshenko's correction for shear in vibrating beams. J. Phys. Appl. Phys. 1975; 8(16):1927.

[17] Chopra AK. Dynamics of structures: theory and applications to earthquake engineering. Prentice-Hall, Upper Saddle River, New Jersey 2001.

[18] Hughes TJR. The finite element method - linear static and dynamic finite element analysis. Prentice Hall Englewood Cliffs, New Jersey 1987; p. 490–567

[19] Anderson JG. Quantitative measure of the goodness-of-fit of synthetic seismograms. Proc. of the 13th World Conference on Earthquake Engineering Conference, Vancouver, Canada 2004; v243.

[20] Boore DM. Notes on relating density to velocity for use in site amplification calculations. http://www.daveboore.com/daves_notes.html 2015.

[21] Mavroeidis GP, Papageorgiou AS. Near-source strong ground motion: characteristics and design issues. Proc. of the Seventh US National Conf. on Earthquake Engineering, Boston, Massachusetts 2002; 21:25.